IMPLEMENTATION OF AN ACTIVE MASS DRIVER FOR INCREASING DAMPING RATIOS OF THE LABORATORIAL MODEL OF A BUILDING

Carlos Moutinho
Álvaro Cunha
Elsa Caetano

University of Porto, Faculty of Engineering (FEUP), Porto, Portugal
e-mail: moutinho@fe.up.pt

This paper describes the experimental work involving a laboratorial implementation of an active system to increase the damping ratios of a plane frame physical model of a building structure of three storeys. For this purpose, the use of an Active Mass Driver commanded by the Direct Velocity Feedback control law is suggested. The study developed to define the maximum control gain based on the classical Root-Locus technique, as well as the analysis of system stability is presented. The efficiency of the proposed control system to achieve pre-defined damping ratios is verified experimentally by observing free decay responses of the system at several natural frequencies before and after control.

Key words: vibration control, active systems, Active Mass Driver, Direct Velocity Feedback, Root-Locus design

1. Introduction

Many Civil Engineering structures have vibration problems in terms of serviceability limit states due to several transient or periodic dynamic loads, e.g., footbridges subjected to pedestrians actions, road and railway bridges excited by traffic loads and tall buildings exposed to wind forces. In these situations, the implementation of control systems can improve the structural performance by reducing the vibration levels to acceptable values. To achieve this, several passive, active, semi-active or hybrid control devices can be used (Chu *et al.*, 2005). This study is addressed to practical cases where the specific use of active systems can be an appropriate solution.

In fact, it is generally accepted that active systems, despite constituting a powerful control scheme, are not an interesting solution to many structural problems, especially when dealing with large structures (Kobori, 2002). This stems from the fact that active control demands sophisticated technology, high costs and high maintenance, and is less reliable than passive systems (Spencer and Nagarajaiah, 2003). However, given the potential of active systems, active control can still be an attractive solution, especially for very flexible systems whose dynamics is dominated by the contribution of several vibration modes (Fujino, 2002). The interest in active control grows when dealing with nonlinear systems and structures that exhibit significant variability in its dynamic parameters (Soong, 1990).

On the other hand, if the problem under analysis involves harmonic vibrations the use of control strategies that conducts to the increasing of damping ratios of the structure is particularly adequate. This is because the amplitude of harmonic responses is strongly influenced by the respective damping ratios, meaning that an appropriate control strategy should be able to increase these damping ratios to predefined values capable to keep the maximum structural response below certain limits. The Direct Velocity Feedback (DVF) control law associated with Root-Locus techniques also constitutes a good strategy that can be used for this purpose since it has the ability to add damping to the structure while providing necessary robustness to the control system (Preumont, 1997). In fact, when some control schemes using collocated pairs of actuators and sensors are used, this strategy leads to unconditionally stable control systems and avoids spillover errors due to unmodeled higher frequency modes (Preumont and Seto, 2008). However, if an Active Mass Driver is used, the control system is no longer unconditionally stable and it may destabilize itself, particularly for high gains (Moutinho, 2008).

In this context, the main objective of this work is to demonstrate how active control can be used to reduce harmonic vibrations in structures using the strategy just described. Although based in simple concepts, this article systematizes the steps and the methodology needed to its real implementation.

2. Review of theoretical background

2.1. Collocated versus non-collocated control

It is well established in theory of system dynamics that in presence of a SISO system, if the actuator and sensor are collocated, i.e., positioned at the same point and measuring in the same direction, the transfer function that relates the system Input and Output has alternating imaginary poles and zeros.

This property is very important in the context of control systems because it ensures that the closed-loop poles of the controlled system remain entirely within the left-half complex plane even if in the presence of uncertainty or variability of the system parameters (Preumont and Seto, 2008). In this case, it is said that the system is robust with respect to stability and the general shape of the Root-Locus plot of such a system is characterized by having several nice stable loops (Ogata, 2009). On the other hand, in the case of non-collocated systems, the pole-zero alternating property is no longer guaranteed, and so there is an effective possibility of achieving system instability in using high control gains. Figure 1 shows a typical view of the Root-Locus diagram of both situations when using a pure derivative controller (same as Direct Velocity Feedback) which has the effect of adding a zero in the open-loop transfer function (represented at the origin of the real/imaginary axis).
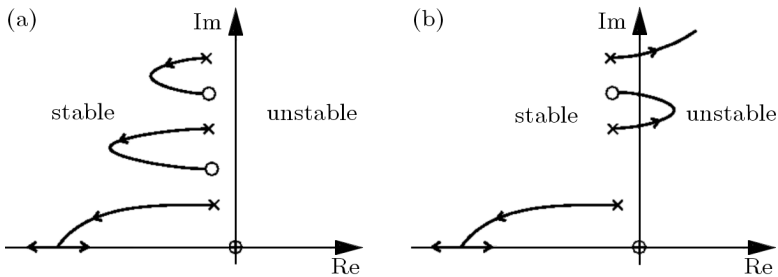

Fig. 1. Root-Locus diagram for (a) collocated and (b) non-collocated control system

2.2. Case of a control system using an Active Mass Driver

One of the most widely known actuation systems used to apply control actions in civil structures is the Active Mass Driver (AMD) which enables generation of inertial forces between the structure and the mass of the device. The main advantage of this control system consists in avoiding external connections from the structure to the ground which, in most of the cases, are undesirable from the architectural point of view. Although AMDs constitute an interesting solution for many practical situations, some design issues must be carefully observed. In fact, AMDs do not correspond to a collocated control system because, although the actuator is positioned in the same location as the measurement point, the force generated with this device is applied at two different points. This effect can be clearly seen in Fig. 2 which represents the model of an AMD integrated with a single degree-of-freedom structure. In this case, the control force is calculated according to the structure response

in correspondence with x_1, being applied as a pair of forces at the degrees-of-freedom related to x_1 and x_2.
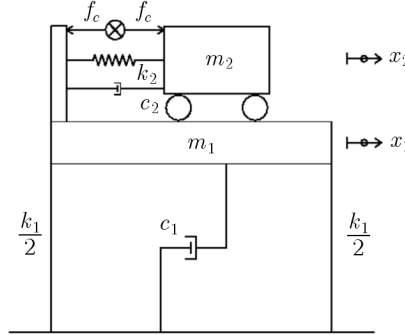

Fig. 2. SDOF structure with an Active Mass Driver

The problem with this scheme is due to the reaction force that goes to the inertial mass which is contrary to the direction of control action. As a consequence, at least one close-loop pole moves in the direction of the unstable region of the complex plane, causing system instability above a certain gain level (Moutinho, 2008).

In order to analyze this situation, the Root–Locus diagram of general case of a multi-degree-of-freedom structure controlled by an AMD using Direct Velocity Feedback is represented in Fig. 3a. As in the previous case, it is clear that the system is potentially unstable for a certain level of gain (g_{max}). To minimize this problem, a large gain margin is desirable, which can be achieved by increasing the damping ratio of the AMD, i.e., moving the respective open-loop pole to the left side. As a result, it is possible to mobilize extra gain and extra damping in the vibration modes of the structure.

Another important issue about the use of AMDs is related to its natural frequency. In the case of Fig. 3a, the open-loop pole associated with the AMD is the lowest frequency pole of the system. This is why the vibration modes of the structure describe increasing damping loops, being the instability conditioned by dynamics of the AMD. On the other hand, if the natural frequency of the AMD is greater than the first natural frequency of the original structure, a zero-pole flipping is observed in the intermediate open-loop poles of the structure, as shown in Fig. 3b. This is disastrous because the damping ratios of the vibration modes with frequencies below the frequency of the AMD decrease as the gain increases. As a consequence, in the Root-Locus diagram, the close-loop poles associated with these modes have loops with departure angles in the direction of the unstable region, and the AMD loop describes a

stable trajectory. Moreover, if the structure is lightly damped, it is necessary just a small gain to get the system unstable by one of these modes.
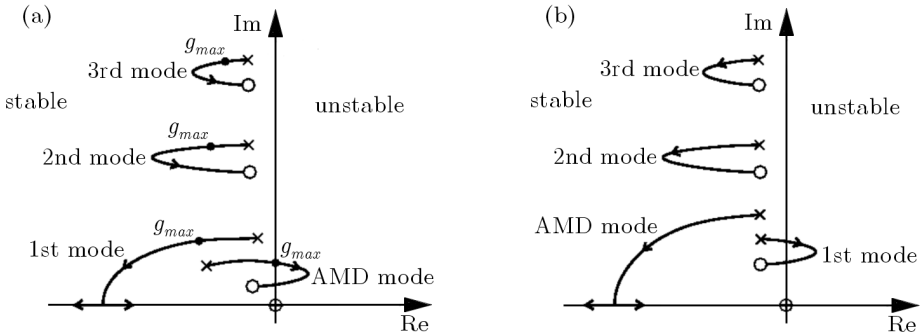

Fig. 3. Root-Locus diagram of a controlled structure using an AMD with (a) low and (b) high frequency

As a summary , it should be emphasized that an ideal AMD used to control a structure should have a high damping in order to get a larger gain margin and mobilize extra damping into the system, and should have a natural frequency below the first natural frequency of the original structure to avoid instability of the lower vibration modes.

3.   Characterization of the experimental control system

3.1.   Description of the physical model, equipments and instrumentation

This section describes the laboratorial implementation of an AMD used to reduce harmonic vibrations in a plane frame physical model, by artificially increasing its initial damping ratios by means of this device. For this purpose, it was developed a model of a shear building structure with 3 storeys which was supported in a shaking table, and a small Active Mass Driver to control vibrations, as shown in Fig. 4.

The physical model is composed by 3 rigid iron masses connected to each other and to the base through aluminum columns. The total mass of each level including the iron mass, mass of the aluminum connections, mass of the sensor and the mass of each half part of the support columns is $m_1 = 15.16\,\mathrm{kg}$, $m_2 = 15.16\,\mathrm{kg}$ and $m_3 = 12.76\,\mathrm{kg}$, corresponding to the 1st, 2nd and 3rd floors, respectively. The aluminum columns have $400\,\mathrm{mm}$ of height, $120\,\mathrm{mm}$ of width and $7\,\mathrm{mm}$ of thickness, and are clamped at each level and at the base. The aluminum modulus of elasticity was evaluated at about $60\,\mathrm{Gpa}$.

Fig. 4. General view of the experimental setup

In order to excite the system with harmonic loads, the physical model was fixed on a shaking table composed of a sliding platform connected to an electromagnetic shaker powered by a current amplifier (see Fig. 5a) which was specially developed to this test. The total mass mobilized at the base of the model including the platform mass of the shaking table, the moving mass of the electromagnetic shaker, the support mass of the model, the mass of the sensor and the mass of each half part of the support columns is $m_0 = 40.51$ kg.
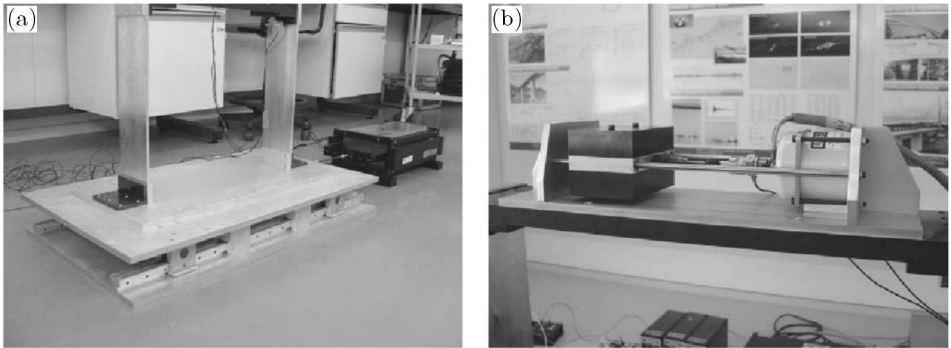

Fig. 5. (a) Detail of the shaking table and (b) detail of the AMD

To control vibrations in the physical model, an Active Mass Driver was installed at the top level. This device is composed of an active 2.89 kg mass, which slides with low friction through 2 circular metallic threads connected to the AMD body which has total mass of 2.65 kg (see Fig. 5b). The active mass is connected to a small electromagnetic shaker which is responsible for application of inertial forces between the active mass and the structure. The

axis of this electromagnetic shaker has a spring of stiffness $k = 3840\,\text{N/m}$ causing damped harmonic motion of the active mass when left in free vibration.
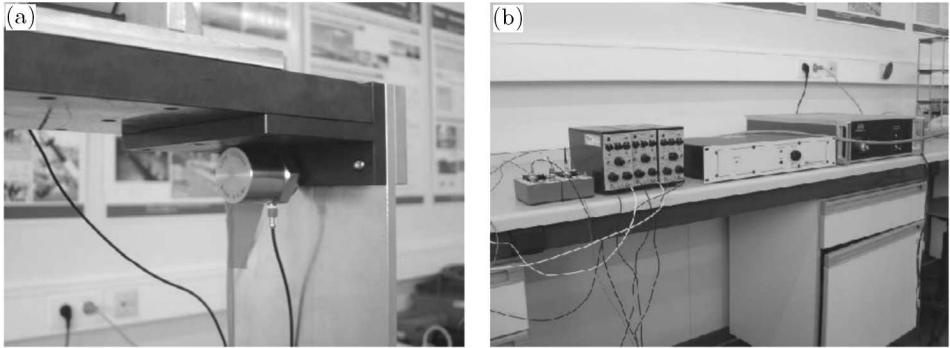

Fig. 6. (a) Detail of the accelerometer (b) signal conditioners and power amplifiers

The system response was continuously measured with accelerometers positioned at the base of the model, at each floor and at the active mass of the AMD (see Fig. 6a). The force developed between the active mass of the AMD and the top level was also measured with a small load cell. The electric current generated by the table shaker and by the AMD shaker was also observed in order to monitor the force applied with these devices. Figure 6(b) shows the power amplifiers of the shaking table and the AMD, and the signal conditioners of the accelerometers. All the transducers mentioned before, as well as the electromagnetic shakers, were operated by a digital computer working with LabVIEW$^{\text{TM}}$ package software, using an acquisition board which performs the signal analog/digital conversion. A Fourier analyzer was also used in the identification of the modal parameters of the structure.

$$\mathbf{M} = \begin{bmatrix} 40.51 & 0 & 0 & 0 & 0 \\ 0 & 15.16 & 0 & 0 & 0 \\ 0 & 0 & 15.16 & 0 & 0 \\ 0 & 0 & 0 & 15.41 & 0 \\ 0 & 0 & 0 & 0 & 2.89 \end{bmatrix}$$

$$\mathbf{K} = \begin{bmatrix} 74.50 & -74.50 & 0 & 0 & 0 \\ -74.50 & 149.00 & -74.50 & 0 & 0 \\ 0 & -74.50 & 149.00 & -74.50 & 0 \\ 0 & 0 & -74.50 & 78.34 & -3.84 \\ 0 & 0 & 0 & -3.84 & 3.84 \end{bmatrix}$$
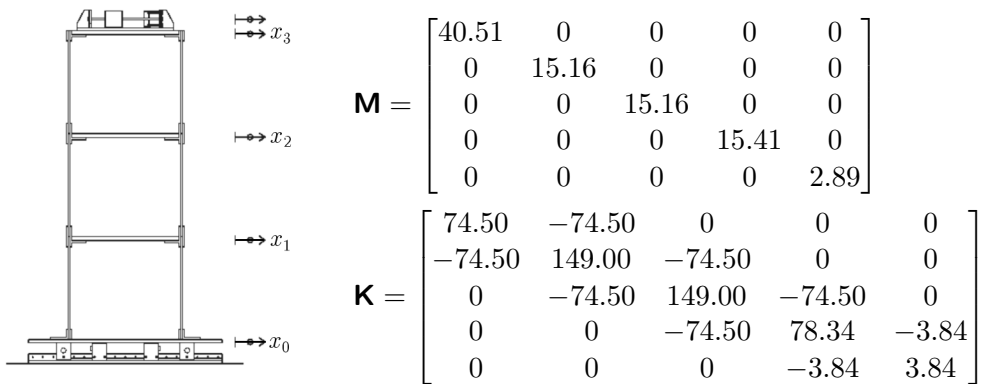
Fig. 7. Identification of degrees-of-freedom of the structure and corresponding mass and stiffness matrices

Taking into account the description of the physical model and data mentioned previously, the mass and stiffness matrices of the laboratorial structure were defined in correspondence with the degrees-of-freedom shown in Fig. 7. These matrices were used in analytical calculations discussed in the next Sections.

3.2. Identification of the modal parameters of the system

In order to identify the modal properties of the system, in particular, the natural frequencies, mode shapes and damping ratios, the model was subjected to several tests and the experimental values were compared with the analytical ones obtained from the numerical model defined in the previous Section (with the exception of damping ratios which can only be evaluated via experimental tests).

The natural frequencies of the system were evaluated with the help of the Fourier analyzer. In this case, FRFs were obtained experimentally by relating the input force applied at the base of the model by the shaking table and the output accelerations measured at several degrees-of-freedom. For this purpose, a frequency range from 0 to 25 Hz was stipulated, and the average of 5 FRFs estimates was considered. Each FRF was estimated based on time series with an acquisition time of 16 s, which means that the frequency resolution achieved is 0.0625 Hz.

Figure 8 shows the magnitude of the FRF obtained, relating the input force at the base of the model and the output acceleration at the top floor. The natural frequencies of the system are clearly identified by the peaks on the graph and their values, as well as the analytical ones, are listed in Table 1.
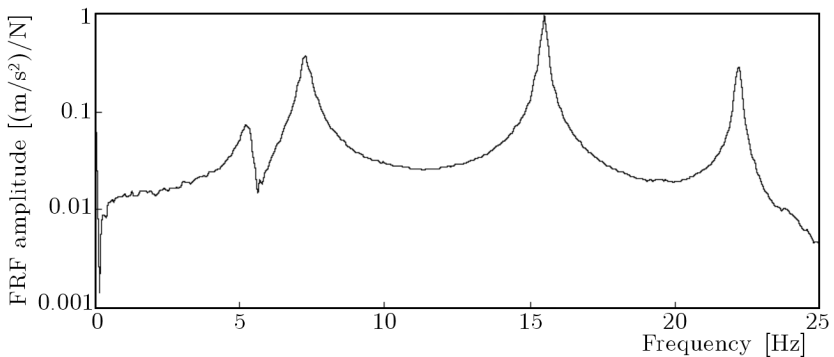

Fig. 8. FRF relating the input force at the base of the model and the output acceleration at the top floor

Table 1. Identified versus analytical natural frequencies

Frequency	Identified [Hz]	Calculated [Hz]
1	5.50	5.45
2	7.35	7.35
3	15.50	14.60
4	22.50	22.25

The method used to identify the vibration mode shapes was simply exciting the structure at resonant frequencies at the base of the model using the shaking table and measuring the amplitude and phase shift of the system response at several degrees-of-freedom. This method is adequate to be applied to small models and gives excellent results because when the structure is subject to a harmonic force with the excitation frequency equal to the natural frequency of the system, the contribution of other vibration modes is negligible when compared with the resonant mode.

Figure 9 shows the graphical representation of the mode shapes in correspondence with the natural frequencies indicated in Table 1. An excellent agreement can be observed between the identified and calculated mode shapes in the same manner as it was observed with the natural frequencies. This means that the analytical model accurately represents the system properties in terms of mass and stiffness.
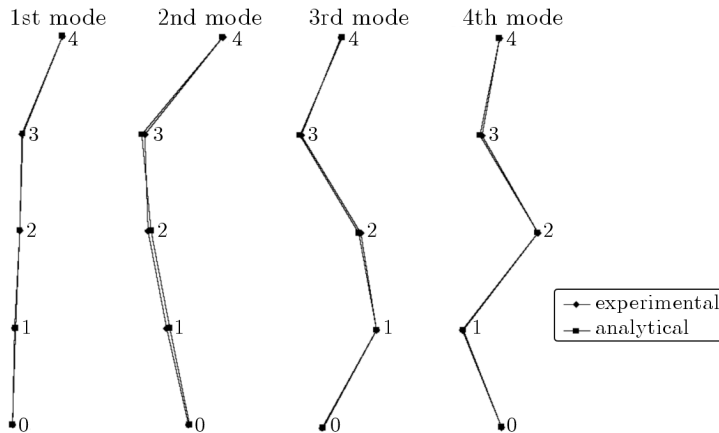

Fig. 9. Identified versus analytical mode shapes

To characterize completely the system parameters, it was necessary to evaluate the damping properties of the structure. In this case, the method used

consists in exciting the physical model with a harmonic force of frequency equal to any of those that were identified as the natural frequencies of the system. By suddenly stopping the excitation, it is easy to measure the free vibration response and estimate the respective damping ratio by analyzing the free decay response envelope, given by the equation $y = A \exp(-\zeta \omega t)$ (Chopra, 2006).

This procedure was adopted to estimate the modal damping ratios of several vibration modes of the physical model. The results obtained are summarized in Table 2, and the time series indicating the system response for each natural frequency are plotted in Fig. 10. Notice that the study of this equation applied to different sets of time intervals allows concluding that the modal damping ratios vary slightly with the displacements amplitude. For this reason, their values were estimated in an intermediate range of the structure response, corresponding approximately to the mean value of the damping ratio.

Table 2. Identified modal damping ratios

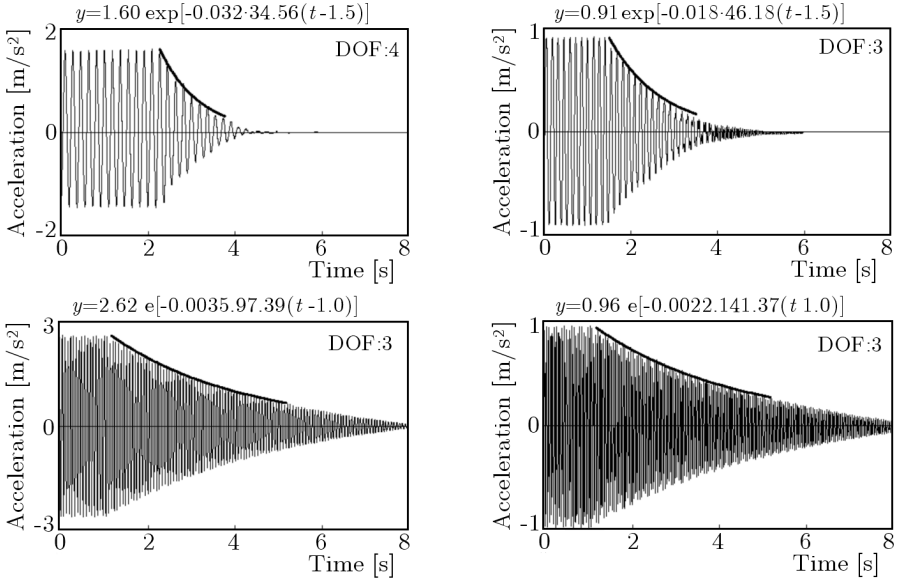| Mode	Identified frequency [Hz]	Modal damping ratio [%]
1	5.50	3.20
2	7.35	1.80
3	15.50	0.35
4	22.50	0.22

Fig. 10. Free vibration responses and the estimated decay envelopes

Based on the modal damping ratios indicated in Table 2, the damping matrix of the system was evaluated using the superposition of modal damping matrices [kg/s] (Chopra, 2006), resulting

$$\mathbf{C} = \begin{bmatrix} 35.30 & -3.74 & -11.47 & -16.11 & -3.99 \\ -3.74 & 7.82 & -0.94 & -1.91 & -1.23 \\ -11.47 & -0.94 & 10.23 & 2.91 & -0.73 \\ -16.11 & -1.91 & 2.91 & 15.00 & 0.11 \\ -3.99 & -1.23 & -0.73 & 0.11 & 5.85 \end{bmatrix}$$

4. Implementation of active control

4.1. Description of the control system

The objective of the control system is to reduce vibration levels of the physical model, when it is excited by harmonic loads. When the frequency of excitation is equal to any of the natural frequencies of the structure, i.e., when the resonance occurs, the system may experience large amplitude motion, depending on the damping ratio of the respective vibration mode. Therefore, an appropriate control strategy should be able to increase the system damping, causing a significant reduction in the structural response. As it is known, when the resonance occurs the amplitude of the dynamic system response is obtained by multiplying the static response by $1/2\zeta$ (being ζ the damping ratio), which suggests that, if the static response is known, the damping ratio should be chosen in order to keep the dynamic response below certain pre-defined limits.

As seen before, the modification of the characteristics of the structure in terms of the modal damping ratio can be obtained using an Active Mass Driver commanded by a derivate controller. The definition of control gains can be studied using the Root-Locus method which also allows evaluating the system stability. An important issue that must be initially considered is the location of the actuator system. The main rule is that the actuator should not be positioned at the point where the significant vibrating modes have reduced modal components.

Using the described control scheme, a real control system was implemented in the plane frame physical model composed of an AMD positioned at the top floor to reduce the vibrations caused by a harmonic excitation applied by the shaking table. The system response at the top floor is continuously measured using an accelerometer connected to the signal conditioner which performs conversion of the accelerations into velocities by integrating the signal from the

transducer. At each time instant, the control force is calculated by multiplying the value of the velocity by a pre-defined gain g and applied to the structure by the AMD shaker connected to the respective power amplifier.

The block diagram of this close-loop control system is represented in Fig. 11. The transfer function $G(s)$ was obtained directly from the system characteristics described in the previous Section, relating the system input/output at the top floor (DOF no. 3).
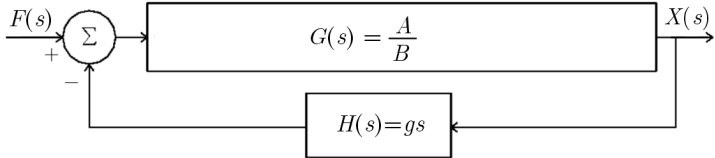
$A = 0.065s^8 + 0.268s^7 + 1395s^6 + 4711s^5 + 6.46\text{E}6s^4 + 1.53\text{E}7s^3 + 2.88\text{E}9s^2 + 2.99s + 16$

$B = s^{10} + 5.06s^9 + 2.79\text{E}4s^8 + 1.21\text{E}5s^7 + 2.20\text{E}8s^6 + 7.41\text{E}8s^5 + 5.13\text{E}11s^4 + 9.41\text{E}11s^3 + 3.41\text{E}14s^2 + 6.42\text{E}6s + 110$

Fig. 11. Block diagram of the closed-loop control system

4.2. Root-Locus design

The Root-Locus diagram of this control system is represented in Fig. 12. This plot clearly shows the advantages of this method to design AMDs, because even if no previous information was available, looking at this diagram, it is possible to immediately conclude that (i) the system has four natural frequencies slightly damped because the open-loop poles are close to the imaginary axis; (ii) the system is unstable for high gains because in this situation there are close-loop poles in the unstable region; (iii) there is a small gain margin until instability is reached because the AMD has relatively low damping; (iv) when the gain increases from zero, the damping ratios of the vibration modes increase, despite the natural frequencies remain approximately the same.

The choice of the control gain affects simultaneously all the close-loop poles locations, which means that it is not possible to select the characteristics of each vibration mode individually. For this reason, when Root-Locus method is used, it must be selected the dominant close-loop pole as the one that contributes more significantly to the system response. The gain is adjusted to move this pole to a more convenient position, conditioning the locations of the other poles. In the case of the present plane frame physical model, when the gain increases, all the modal damping ratios increase in correspondence with a specific gain value, which is fixed when the target close-loop pole reaches the desired location in correspondence with the pre-defined damping ratio.
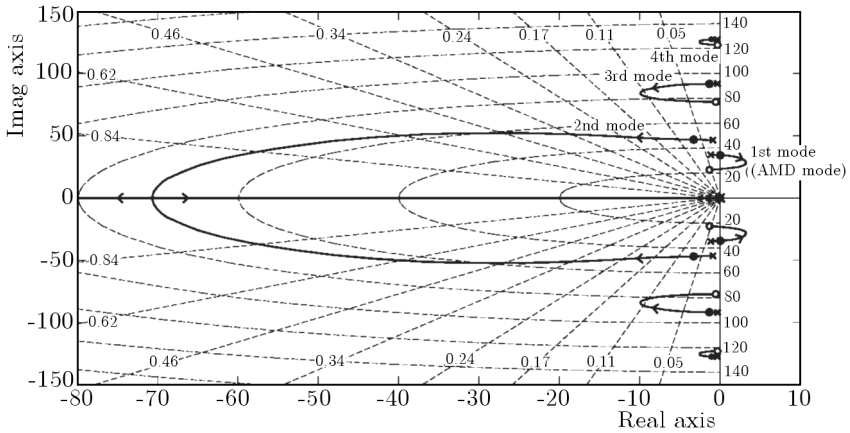
Fig. 12. Root-Locus diagram of the plane frame controlled by an AMD

In the case of this test, the AMD developed has a relatively low damping ($\zeta_{TMD} \approx 3.2\%$) due to construction issues, which limits the efficiency of this control system. However, even in this situation it is possible to significantly increase the damping ratios of the structure to maximum values according to the maximum achievable gain $g = 82$, until instability occurs. If this gain is selected, the close-loop poles move to the locations marked with small dots in the Root-Locus diagram, which are in correspondence with the new damping ratios listed in Table 3.

Table 3. Calculated modal damping ratios for control gains $g = 0$ and $g = g_{max} = 82$

Mode	ζ_i [%] for $g = 0$ (without control)	ζ_i [%] for $g = 82$ (control with g_{max})
1	3.20	–
2	1.80	7.09
3	0.35	1.44
4	0.22	0.44

4.3. Experimental results

In order to experimentally verify the efficiency of the described control system, the damping ratios of the physical model were evaluated after switching on the AMD with an intermediate gain $g = 60$. In this circumstance, the model was excited with a harmonic load with a frequency in correspondence with
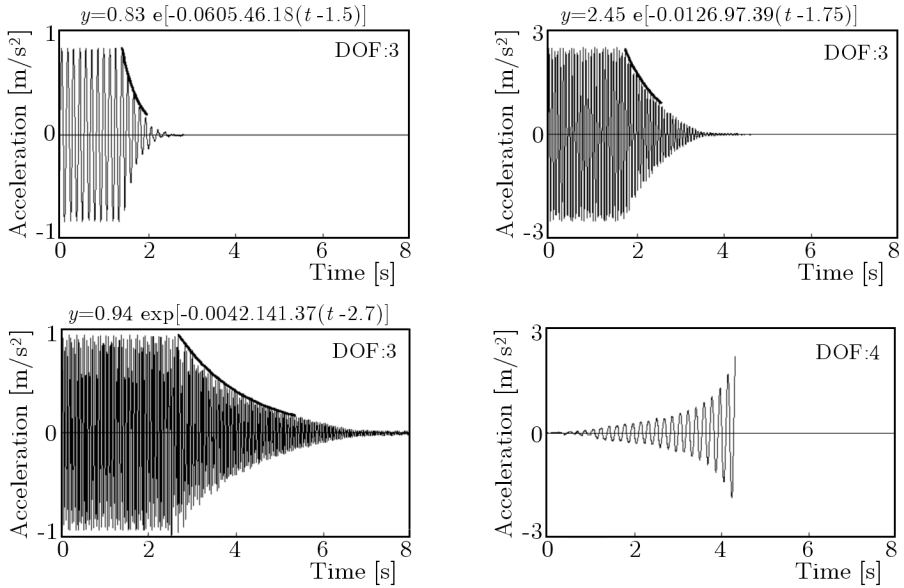
Fig. 13. Free vibration responses and estimated decay envelopes for control gain
$g = 60$ and system response for unstable control gain $g = 150$

the identified natural frequencies of the system and, after stopping the excitation, the free decay response was recorded in order to evaluate the respective modal damping ratio. The results obtained are represented in Fig. 13 and are summarized in Table 4, where the experimental values are also compared with the analytical ones.

Table 4. Identified versus calculated modal damping ratios for control gain $g = 60$

Mode	Identified [%]	Calculated [%]
1	–	0.83
2	6.05	5.72
3	1.26	1.15
4	0.42	0.38

System instability was also verified when the control gain exceeds its maximum value, by introducing a clearly excessive gain of $g = 150$. As expected, the noise in the sensors was sufficient to excite the system, which became unstable by the uncontrolled harmonic vibration of the structure with the

frequency of the AMD vibration mode. This situation was clearly predicted by the analysis of the Root-Locus diagram plotted in Fig. 12.

5.   Conclusions

This paper describes a laboratorial implementation of an active damping system to reduce vibrations in a 3-DOF physical model subjected to harmonic vibrations. When a resonance occurs, the amplitude of the dynamic response is strongly influenced by the damping ratio of the respective vibration mode. This means that a good control strategy should be able to increase the damping in the system in order to keep its response below certain limits.

For this purpose, an AMD commanded by the Direct Velocity Feedback control law, resulting in a control system that applies an inertial force proportional to the velocity at the control point can be used. However, the use of the AMD constitutes a non-collocated sensor/actuator scheme, causing system instability particularly for high gains. To analyze this problem, the Root-Locus diagram is a powerful method that allows examination of the system stability as well as designing the control gain necessary to reach some structural properties, particularly in terms of damping ratios.

In order to experimentally verify the efficiency of this control system, the physical model was subjected to resonant harmonic loads applied by a shaking table, aiming at the evaluation of several modal damping ratios by analyzing the respective free decay envelopes. It was observed a good agreement between the experimental and analytical results corresponding to a significant increase of the damping ratios of the system with a consequent important reduction of its harmonic response.

References

1. CHOPRA A., 2006, *Dynamics of Structures Theory and Applications to Earthquake Engineering*, 3rd edition, Prentice-Hall

2. Chu S., Soong T., Reinhorn A., 2005, *Active, Hybrid, and Semi-active Structural Control: A Design and Implementation Handbook*, John Wiley & Sons, Ltd.

3. Fujino Y., 2002, Vibration, control and monitoring of long-span bridges – Recent research developments and practice in Japan, *Journal of Constructional Steel Research*, **58**, 71-97

4. Kobori T., 2002, Past, Present and future in seismic response control in civil rngineering structures, *3rd World Conference on Structural Control*, **1**, 9-14

5. Moutinho C., 2008, *Vibration Control in Civil Engineering Structures*, PhD thesis, FEUP

6. Ogata K., 2009, *Modern Control Engineering*, 5th edition, Prentice-Hall

7. Preumont A., 1997, *Vibration Control of Active Structures – An Introduction*, Kluwer Academic Publishers

8. Preumont A., Seto K., 2008, *Active Control of Structures*, John Wiley & Sons, Ltd.

9. Soong T., 1990, *Active Structural Control – Theory and Practice*, Longman Scientific & Technical

10. Spencer Jr. B., Nagarajaiah S., 2003, State of the art of structural control, *Journal of Structural Engineering, ASCE*, **129**, 845-856

Zastosowanie aktywnego układu redukcji drgań do zwiększenia współczynników tłumienia laboratoryjnego modelu budynku

Streszczenie

W pracy opisano badania doświadczalne przeprowadzone na stanowisku laboratoryjnym, których celem była analiza układu aktywnej redukcji drgań zwiększającego współczynniki tłumienia w płaskim, ramowym modelu trzykondygnacyjnego budynku. Cel ten zrealizowano na modelu z inercyjnym układem redukcji drgań sterowanym w prędkościowej pętli sprzężenia zwrotnego. Przedyskutowano problem stateczności modelu metodą linii pierwiastkowych (*Root-Locus*), pozwalającą na określenie maksymalnego dopuszczalnego współczynnika wzmocnienia w układzie sterowania. Skuteczność zaproponowanej metody sterowania ukierunkowanej na uzyskanie żądanych właściwości tłumiących zweryfikowano eksperymentalnie poprzez obserwację spadku amplitudy drgań swobodnych pobudzanych wcześniej przy kilku częstościach własnych modelu z włączonym i wyłączonym układem sterowania.